Relativistic dynamical bistability and adiabatic excitation of strong plasma waves[a)]

Oleg Polomarov[b)] and Gennady Shvets
Department of Physics and Institute of Fusion Studies, The University of Texas at Austin, Austin, Texas 78712

(Received 14 November 2006; accepted 9 January 2007; published online 2 May 2007)

Adiabatic evolution of the nonlinear resonantly driven dynamical system generic to a variety of plasma physics problems, including generation of large-amplitude plasma waves in a plasma beat-wave accelerator, is studied. The properties of the resonant Hamiltonian and the dynamics of its phase space for adiabatically varying parameters are considered. It is shown that the system can exhibit bistability and the Hamiltonian of a bistable system always follows the same trajectory for the adiabatically varying driver regardless of whether the system is excited or left quiescent. Descriptions of the bistability, autoresonance, and their possible combination based on the properties of the resonant Hamiltonian are given. © *2007 American Institute of Physics*.
[DOI: 10.1063/1.2710783]

I. INTRODUCTION

Resonant excitation of nonlinear dynamical systems is a common uniting thread throughout plasma science. Best known examples include resonant beat-wave (BW) excitation of electron plasma waves[1–5] in a plasma beat-wave accelerator (PBWA) and electron cyclotron resonance heating (ECRH) by radio frequency waves.[7–9] Many different nonlinear systems can be described by a generic resonant Hamiltonian

$$H(I,\theta,\tau) = b(\tau)I - cI^2 - a(\tau)\sqrt{2I}\sin\theta, \tag{1}$$

where I and θ are canonical conjugate variables, and a, b, and c are parameters of the system and driver (slowly varying). For PBWA, Hamiltonian (1) can be derived from the quasistatic equation for the normalized electrostatic potential $\Phi = e\phi/mc^2$ of a driven plasma wave in the comoving frame $\tau = \omega_p(t - z/c)$,

$$\frac{d^2\Phi(\tau)}{d\tau^2} = \frac{1}{2}\left(\frac{1 + 2R[1+\cos(\omega\tau+\theta)]}{[1+\Phi(\tau)]^2} - 1\right). \tag{2}$$

Here, $R = (e/mc)^2 E_1 E_2/\omega_1\omega_2$ is the normalized BW amplitude of a pair of linearly polarized laser pulses with electric field amplitudes E_1 and E_2 and the corresponding frequencies ω_1 and $\omega_2 = \omega_1 - \omega_B$. The normalized driver frequency is $\omega = \omega_B/\omega_p$, where $\omega_p = \sqrt{4\pi e^2 n/m}$ is the electron plasma frequency. Expansion of Eq. (2) in slow-varying amplitude $u(\tau)$ and phase $\theta(\tau)$ (e.g., dephasing between the driver and the wave) with $\Phi(\tau) \simeq u(\tau)\cos[\omega\tau + \theta(\tau)] + \cdots$ leads to the system of equations that can be rewritten in a canonical form for conjugate variables $I = u^2/2$ and θ with Hamiltonian (1), where $b = 1 - \omega$ (detuning), $c = 3/16$, and $a = R$ (the driver amplitude).[5,11]

Earlier investigations of the Hamiltonian (1) in Refs. 7 and 11 have revealed an important property of its phase space: depending on the values of a, b, and c, there are either one (elliptic) fixed point or three (two elliptic, one hyperbolic) fixed points. Displacement of the fixed points in the $[I,\theta]$ phase plane, their disappearance or reappearance, change the topology of the phase space. This becomes important for the dynamical systems described by Eq. (1) with slowly varying coefficients. For example, a nonlinear oscillator (a relativistic plasma wave) can be effectively and well-controllably excited by a near-resonant driver (beat-wave) pulse with slowly varying amplitude $a(\tau)$ and frequency $\omega(\tau)$. Two seemingly different approaches to adiabatic excitation of nonlinear oscillations have been theoretically studied. The first approach is the "autoresonant" excitation by slowly decreasing (or "chirping") the *driver frequency* through the exact resonance $b = 0$. This approach does not rely on the topological change of the phase portrait and was shown to be effective for excitation of the plasma waves by a chirped laser beat wave[12,13] and for the ECRH of plasma.[9,10] The second is the "bistability" approach, realized when the *driver amplitude* slowly evolves from zero to a certain above-threshold value, and then back to zero. It does rely on the topological change of the phase space at the threshold $a = a_{cr}$. When the phase-space topology changes from the one with a single elliptic point to that with two elliptic points, the system must cross the separatrix and "choose" (depending on its position in the phase space at the time of the crossing) to be in one of the two accessible regions of the phase space with subsequent adiabatic evolution in one of the two possible bistable wakes. The bistability approach has been applied to ECRH in a uniform magnetic field[6,7] and to BW excitation of strong plasma waves in Refs. 5 and 11.

The main goal of this work is to show that the adiabatic methods of excitation of the nonlinear oscillator with Hamiltonian (1), such as bistability and autoresonance (and their combination), allow highly effective and well-controllable generation of the large oscillation wake with definite amplitude, which does not depend on the shape of the driver pulse.

[a)]Paper WI1 4, Bull. Am. Phys. Soc. **51**, 333 (2006).
[b)]Invited speaker.

The last property can be very useful as it does not require careful designing of the laser (driver) pulse for obtaining the precise wake amplitude, as is the case for the nonadiabatic excitation [with constant parameters of the Hamiltonian (1), see Ref. 2].

II. EVOLUTION OF THE HAMILTONIAN ALONG "SISTER" TRAJECTORIES FOR SLOW VARYING DRIVER

Here, we show that the bistable Hamiltonian (1) possesses an important "conservation" property (overlooked in the previous works on the ECRH), namely, in the adiabatic limit, when the bistability excitation mechanism is used, the value of $H(a)$ at a given amplitude a does not depend on the outcome of the separatrix crossing. The adiabatic limit here implies a vanishingly small rate of change of the driver amplitude, when the nonadiabatic effects due to separatrix crossing[17] can be neglected ($a/T_{\rm osc} \gg da/d\tau$, where $T_{\rm osc}$ is the period of oscillation in the phase space of the slow variables $[I,\theta]$). Specifically, for driver amplitudes $a<a_{\rm cr}$ there are two "sister" trajectories corresponding to the same value $H(I,\theta)\equiv h(a)$ and separated by the separatrix. Here h plays the role of energy in oscillating frame. Repeated separatrix crossings, due to adiabatically varying driver $a(\tau)$, can result in switching from one "sister" trajectory to another, or in staying on the same "sister" trajectory. Nevertheless, in either case, the value of the Hamiltonian is the same and determined only by the driver strength for the given initial condition.[5,11]

A. The properties of the resonant Hamiltonian for constant parameters

We start by reviewing the basic properties of the phase portraits of the dynamical system governed by the Hamiltonian H with constant coefficients a,b, and $c>0$. A particle representing the dynamical system under consideration moves according to the Hamilton equations:

$$\frac{dI}{d\tau}=-\frac{\partial H}{\partial \theta},\quad \frac{d\theta}{d\tau}=\frac{\partial H}{\partial I}. \tag{3}$$

The phase-space trajectories in the $[I,\theta]$ phase plane are the constant energy contours $H(I,\theta)=h$. Let us consider the phase portraits for the three distinct regions of parameters a and b:

(i) For positive $b>0$ ($\omega<1$) and $0<a<a_{\rm cr}$ (when the driver amplitude is smaller than some critical value given below), the system 3 has three fixed points ($dI/d\tau=0, d\theta/d\tau=0$), namely, two stable elliptic points (upper and lower) and one unstable hyperbolic point (see Figs. 1 and 2).

(ii) For $b>0$ and $a>a_{\rm cr}$, there is only one upper stable elliptic point (see Fig. 3), as well as for the case

(iii) $b\leq 0$ (for $\omega\geq 1$) and for any a (see Figs. 4 and 5).

With a replacement $I=u^2/2$, the hyperbolic u_g and the lower elliptic u_l points are the maximal and minimal non-negative roots of $bu-cu^3-a\sin \pi/2=0$, correspondingly. The upper elliptic point $u_{\rm up}$ is the non-negative root of $bu-cu^3-a\sin 3\pi/2=0$. The critical driver amplitude $a_{\rm cr}$ corresponds to merging and annihilating of the hyperbolic and lower elliptic points and is given by $a_{\rm cr}=2/3\sqrt{b^3/3c}$. The critical driver amplitude corresponds to critical slow ampli-

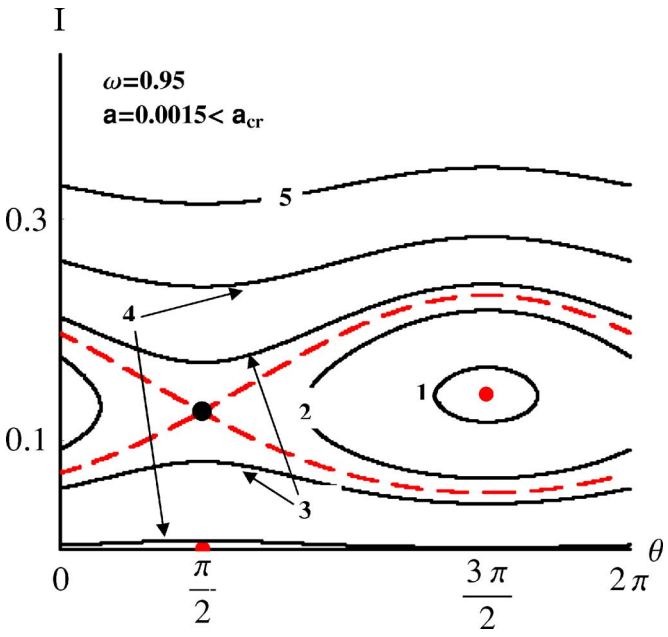

FIG. 1. (Color online) The phase portrait $[I=u^2/2,\theta]$ of trajectories of $H(I,\theta)=h$ for different values of the Hamiltonian h. The case $a=0.0015<a_{\rm cr}$ and $\omega=0.95$ ($b=1-\omega$). Black lines are phase space trajectories: "1" corresponds to $h=0.004$, "2" to $h=0.003$, "3" to $h=0.0022$, "4" to $h=0.0002$, and "5" to $h=-0.004$; trajectories marked by "3" and "4" are the corresponding "sister" trajectories. The red dashed line is the separatrix. The black dot is the hyperbolic point and the red dots are the upper (encircled by trajectory "1") and lower elliptic points.

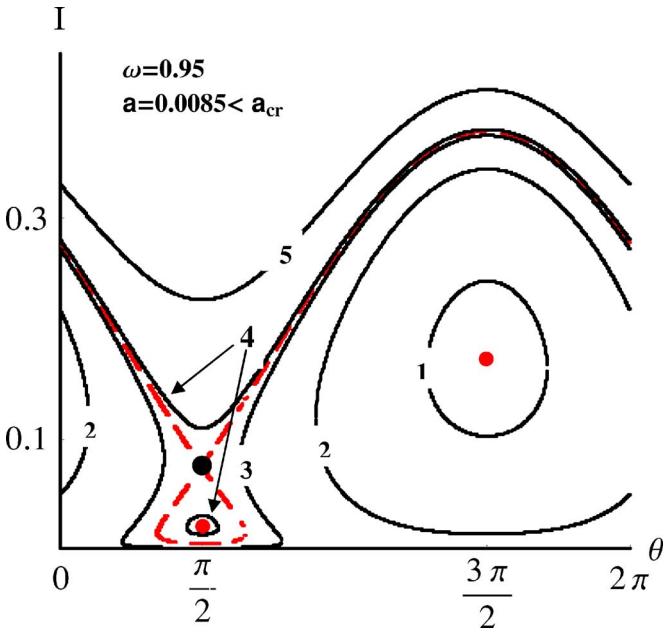

FIG. 2. (Color online) The phase portrait for the case $a=0.0085<a_{\rm cr}$ and $\omega=0.95$. All definitions are the same as in Fig. 1. Trajectories are as follows: "1" corresponds to $h=0.007$, "2" to $h=0.002$, "3" to $h=-0.0004$, "4" to $h=-0.00075$, and "5" to $h=-0.005$; trajectories "4" represent "sisters."

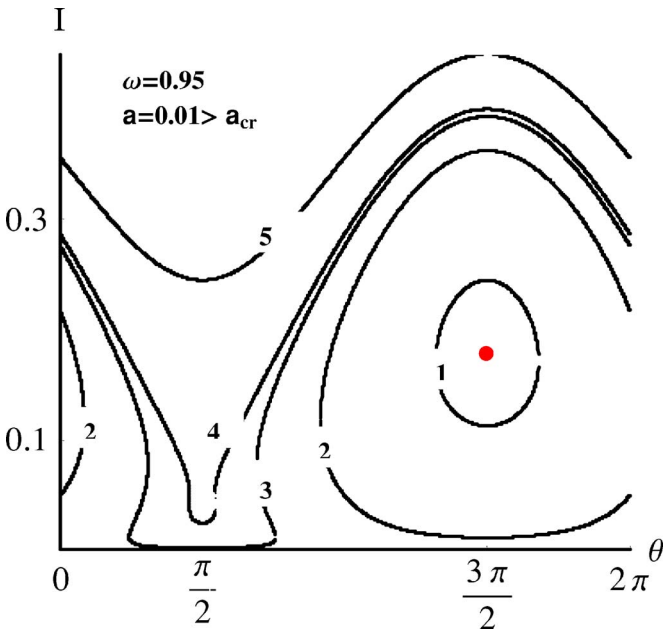

FIG. 3. (Color online) The phase portrait for the case $a=0.01>a_{cr}$ and $\omega=0.95$. All definitions are the same as in Fig. 1. Trajectories are as follows: "1" corresponds to $h=0.008$, "2" to $h=0.002$, "3" to $h=-0.0005$, "4" to $h=-0.0011$, and "5" to $h=-0.006$.

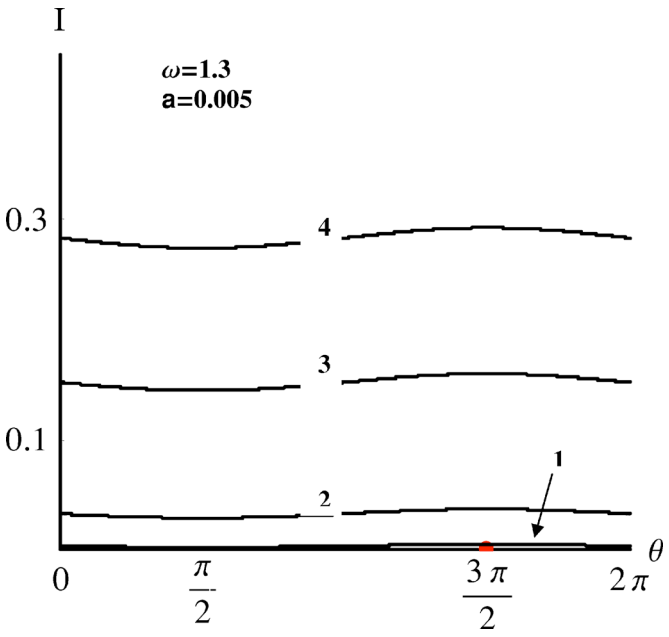

FIG. 5. (Color online) The phase portrait for the case $a=0.005$ and $\omega=1.3$. All definitions are the same as in Fig. 1. Trajectories are as follows: "1" corresponds to $h=-0.001$, "2" to $h=-0.01$, "3" to $h=-0.05$, and "4" to $h=-0.1$.

tude $u_{cr}=\sqrt{b/3c}$. Also, it can be shown that the fixed points are ordered as $0<u_l<\sqrt{b/3c}<u_g<\sqrt{b/c}<u_{up}$.

Depending on the particular value of the driver amplitude a and energy h, the trajectory of the system can librate ($\Delta\theta<2\pi$) or rotate ($\Delta\theta\geq 2\pi$) around either of the elliptic points (or point for $a>a_{cr}$, or $b\leq 0$), or can rotate around all fixed points, as is seen from Figs. 1–5. The trajectories are ordered as follows.

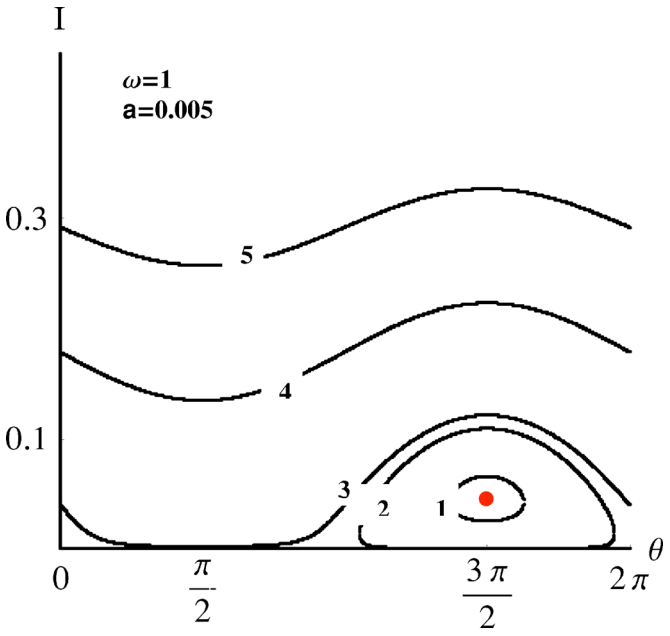

FIG. 4. (Color online) The phase portrait for the case $a=0.005$ and $\omega=1$. All definitions are the same as in Fig. 1. Trajectories are as follows: "1" corresponds to $h=0.001$, "2" to $h=0.0001$, "3" to $h=-0.0003$, "4" to $h=-0.006$, and "5" to $h=-0.016$.

Case (i): $b>0$ and $a<a_{cr}$, see Figs. 1 and 2, for (a) $h>H(u_{up},3\pi/2)$, there is no trajectories at all; (b) for $H(u_g,\pi/2)<h<H(u_{up},3\pi/2)$, there is only one solution to $H(u,\theta)=h$ and trajectories with different h are librating or rotating around the upper elliptic point u_{up}; (c) for $H(u_l,\pi/2)<h<H(u_g,\pi/2)$ for each h, there are always two solutions of $H(u,\theta)=h$ with the same h ("*sister" trajectories*)—one solution is oscillating around the lower elliptic point u_l and the other solution is rotating around all fixed points; (d) for $h<H(u_l,\pi/2)$ for each h, there is again only one solution of $H(u,\theta)=h$ which rotates around all fixed points and lies above all previously considered trajectories. Note, the existence of "sister" trajectories, or multivalue solutions of $H(u,\theta)=h$, as in the case (c), is of crucial importance for the possibility of the bifurcation phenomenon, which can lead to bistable behavior of the solutions of system 3.

Case (ii): $b>0$ and $a>a_{cr}$, see Fig. 3, for (a) $h>H(u_{up},3\pi/2)$, there are no trajectories at all, and for (b) $h<H(u_{up},3\pi/2)$, all trajectories are librating or rotating around the only existing upper elliptic point.

Case (iii): $b\leq 0$, as is shown in Figs. 4 and 5, the phase portraits of system 3 are similar to the case $b>0$ and $a>a_{cr}$ containing only one stable elliptic point u'_{up}. There are no trajectories for $h>H(u_{up},3\pi/2)$, and for $h<H(u_{up},3\pi/2)$ all solutions $H(u,\theta)=h$ are single-valued and oscillate around the u'_{up}. Importantly, the stable elliptic point u'_{up} for nonpositive b becomes the upper elliptic point u_{up} if b goes into the region of positive values. Note, the transformation of the elliptic point of the case $\omega\geq 1$ (when $b\leq 0$) into the upper elliptic point of the case $\omega<1$ (when $b>0$) is necessary for the so-called autoresonant excitation of the large-amplitude u oscillation.

Another important property of the Hamiltonian (1) is the existence for $b>0$ and $a<a_{cr}$ of the separatrix, or the improper solution of $H(u,\theta)=H(u_g,\pi/2)$ with trajectory going through the hyperbolic point, see Figs. 1 and 2. The separatrix is an improper trajectory as the time of full oscillation along it is infinite. The lower branch of the separatrix "separates" the regions around the lower and upper elliptic points from each other, and the upper branch of the separatrix isolate the region of the upper elliptic point from the outer region where trajectories rotate around all fixed points. Note, the separatrix moves with varying a (as well as all fixed points). Indeed, for $a\to 0$ both branches of the separatrix approach each other and the line $u=\sqrt{b/c}$; meanwhile for $a\to a_{cr}$, the lower separatrix branch tightened to a point around the hyperbolic point u_h and for $a=a_{cr}$ the entire separatrix disappears.

B. Properties of the resonant Hamiltonian for the adiabatically varying driver

Having reviewed the relevant features of the phase portraits of the stationary $H(I,\theta)$, we state a rather remarkable property of the "sister" trajectories: their oscillation periods are identically equal:

$$T_1(h)=T_2(h), \tag{4}$$

where 1 and 2 label, respectively, the lower and the upper trajectories. Equation (4) holds for any values of a, b, and c for which "sister" trajectories exist. Equation (4) is proven by integration of the governing system of Eqs. (3) (see Ref. 16), resulting in

$$T_1=T_2\equiv\frac{4}{c\sqrt{(I_4-I_2)(I_3-I_1)}}\mathbf{K}\left[\frac{(I_4-I_3)(I_2-I_1)}{(I_4-I_2)(I_3-I_1)}\right], \tag{5}$$

where $\mathbf{K}[m]$ is the complete elliptic integral[18] of the first kind.

When energy h evolves adiabatically in time, any given phase-space trajectory is deformed so as to preserve its adiabatic invariant $J=\frac{1}{2\pi}\oint Id\theta$.[14] The two "sister" trajectories change so as to remain the solutions of the $H(u,\theta,\tau)=h_{1,2}(\tau)$ and also to conserve the corresponding adiabatic invariants $J_{1,2}$. For fixed b and c actions $J_{1,2}\equiv J_{1,2}(h,a)$ are functions of slowly evolving driver amplitude a. *Remarkably*, $h_1(\tau)=h_2(\tau)$. To prove this statement, note that from $J(h,a)_{1,2}=\text{const}_{1,2}$ it follows that

$$\frac{dh_{1,2}}{da}=-\frac{\partial J_{1,2}}{\partial a}\Big/\frac{\partial J_{1,2}}{\partial h}. \tag{6}$$

Accounting for the relationship for the "sister" trajectories, proven in Ref. 16,

$$J_1(h,a,b,c)-J_2(h,a,b,c)=b/c, \tag{7}$$

yields that $\partial J_1/\partial h=\partial J_2/\partial h$ and $\partial J_1/\partial a=\partial J_2/\partial a$ because the right-hand side (RHS) of Eq. (7) is independent of h and a. Finally, combining these equalities with Eq. (6) implies that the rates of change of energy h with varying driver amplitude a are the same for both "sister" trajectories,

$$dh_1/da=dh_2/da. \tag{8}$$

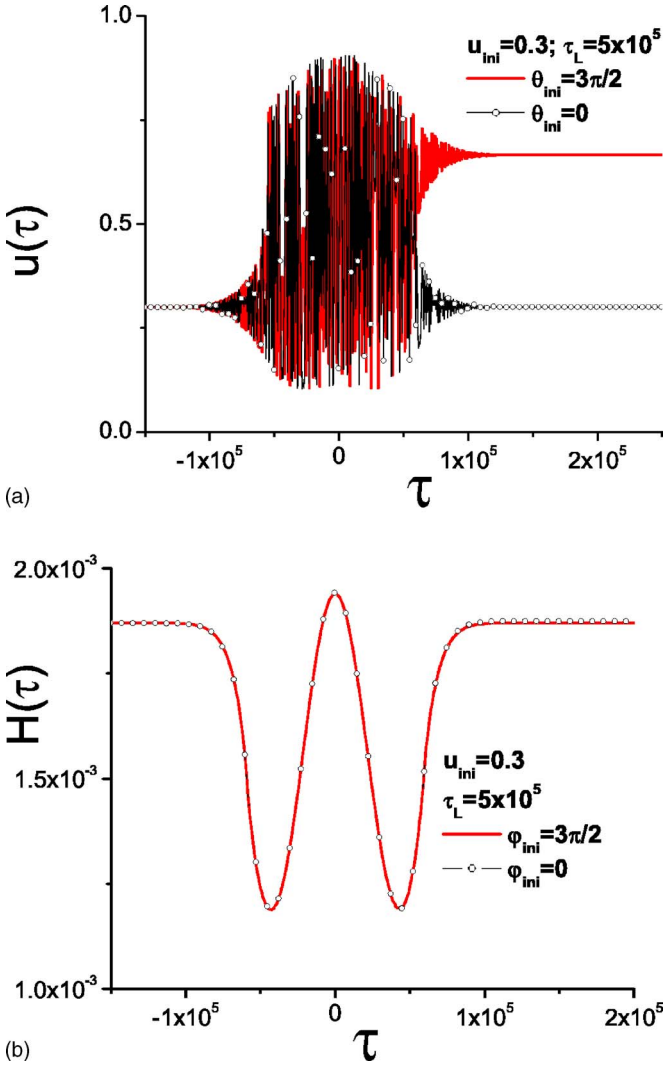

FIG. 6. (Color online) The slow amplitude $u(\tau)$ and the energy $H(\tau)$ along the trajectories $u(\tau),\theta(\tau)$ with different initial conditions for adiabatically varying diver $a(\tau)$.

Therefore, if at some time τ two representative particles occupy "sister" trajectories, they will remain on the equal-energy ("sister") trajectory for as long as the driver $a(\tau)$ is changing adiabatically.

To be specific, assume that the system initially resides on the lower "sister" trajectory. Consider a driver amplitude increasing past the certain value a_s for which the system crosses the separatrix *into* the basin of the upper elliptic point. When the driver amplitude reaches the maximum and decreases again to $a=a_s$, the system crosses the separatrix again *from* the basin of the upper elliptic point. It can now end up either on its initial (lower) trajectory, or on its "sister" upper trajectory. From that point on, the system remains on the chosen trajectory for $a<a_s$. Neglecting small nonconservation of the adiabatic invariant during the separatrix crossing,[17] we conclude from Eq. (8) that the energy of the system remains the same regardless of whether it returns to its initial trajectory or is excited into the "sister" trajectory.

To confirm these analytic predictions, we have numerically integrated Eq. (3) with the variable driver amplitude $a(\tau)=a_m\exp(-\tau^2/\tau_L^2)$, where $a_m=0.03>a_s$ and $\tau_L=5\times 10^5$.

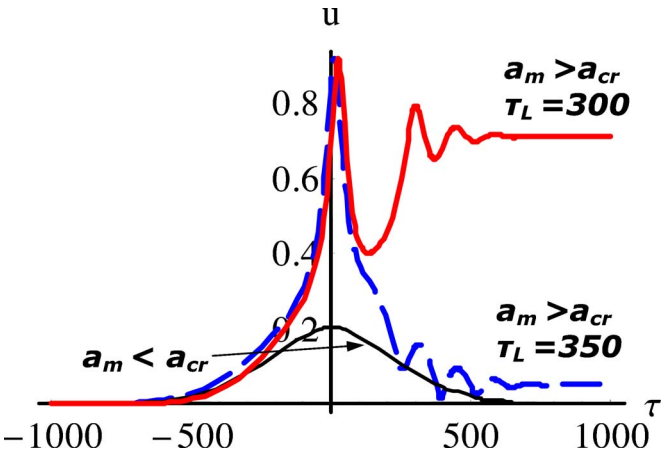

FIG. 7. (Color online) The oscillation amplitude vs normalized time for bistability. (i) $a_m > a_{cr}$: red line, large wake ($\tau_L = 300$); blue, small wake ($\tau_L = 350$). (ii) $a_m < a_{cr}$: black, small wake.

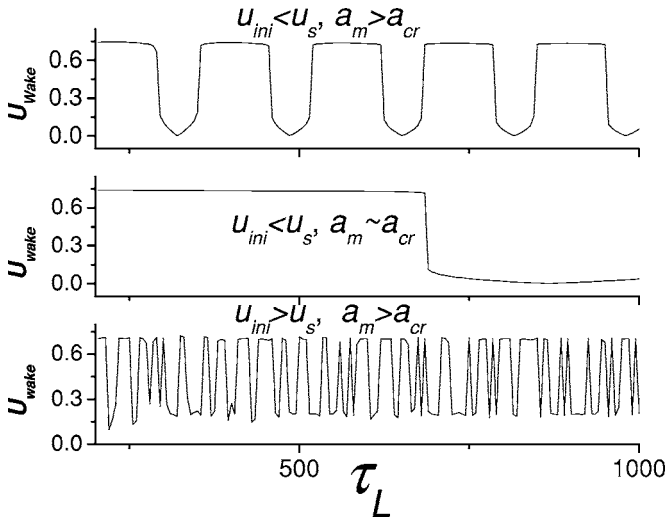

FIG. 8. The wake amplitude u_{wake} vs the driver pulse length τ_L for different initial amplitudes u_{ini} and the same phase $\theta = 0$.

In Fig. 6, the slow amplitudes $u(\tau)$ and the energy $h(\tau)$ corresponding to the initial amplitude $u_{ini} = 0.3$, and two initial phases $\theta = 0$ and $\theta = 3\pi/2$ are plotted. Clearly, the Hamiltonian evolves in the same way along the trajectories that correspond to the same initial value $h_{ini} = h(u_{ini})$ even if these trajectories diverge after a bifurcation: the trajectory with $\theta_{ini} = 3\pi/2$ acquires the final amplitude much larger than initial $u(\tau = +\infty) > u_{ini}$ and the trajectory with $\theta_{ini} = 0$ returns to its initial value $u(\tau = +\infty) = u_{ini}$.

Note, the property of our Hamiltonian to remain the same after a bifurcation is a particular property of our system and is only valid for the case of adiabatically varying driver $a(\tau)$ (not for adiabatically varying detuning).

III. BISTABILITY

Having reviewed the properties of the governing Hamiltonian (1) and its "sister" trajectories, we describe the mechanism of bistability-based excitation of large oscillations and several different regimes of it. As mentioned above, bistability relies heavily on the property of the Hamiltonian to remain equal for the two "sister" trajectories with slow varying driver amplitude $a(\tau)$. Mainly, the bistability can be viewed as a possible transition of the representative oscillation with $[I, \theta]$ from the lower "sister" trajectory to the upper "sister," as these trajectories merge and then disrupt when the driver goes through a_{crit} with ascending and descending amplitude consequently. The time-dependence of the oscillation amplitude $u(\tau)$ for the case of bistability for Gaussian-shape driver $a(\tau) = a_m \exp(-\tau^2/\tau_L^2)$ is shown in Fig. 7. It is seen that for $a_m > a_{cr}$, the wake amplitude acquires only two definite values: (i) large and (ii) small, depending on the driver pulse length (also, the bistable dependence of the wake amplitude versus driver length is clearly seen at Fig. 8). For small driver amplitudes $a_m < a_{cr}$, there is only a small wake amplitude, as in this case the representative oscillation during its adiabatic evolution always remains on the lower sister trajectory and there is no bifurcation.

The magnitude of the oscillation wake behind the driver pulse $[\tau_{wake} \to +\infty,\ a(\tau_{wake}) = 0]$ can be easily calculated in the adiabatic limit by solving a simple algebraic equation $H(I, \theta, a(\tau_{wake})) = h_{ini}$, where h_{ini} is the initial value of the Hamiltonian for $\tau_{ini} = -\infty$ (for initially quiescent plasma $h_{ini} = 0$), as it follows from the above considered adiabatic property of the Hamiltonian (1). For example, for the initially quiescent plasma, the wake amplitude for the adiabatic driver with $a_m > a_{cr}$ only depends on the driver frequency ω, and is given by $u_{wake} = 4\sqrt{2(1-\omega)/3}$, or $u_{wake} = 0$. Also, the wake amplitude does not depend on the driver pulse shape, as long as it is adiabatic ($a/T_{osc} \gg da/d\tau$).

Knowing the two possible outcomes for oscillation amplitudes, it is interesting to investigate the regions of parameters (in our case, the driver pulse length τ_L, initial oscillation amplitude u_{ini}, and phase θ_{ini}) which lead to one of the two possible bistable outcomes. First of all, the dependence of the wake oscillation amplitude on the driver pulse length and phase is drastically different for oscillations with initial amplitudes less and larger than the particular initial ampli-

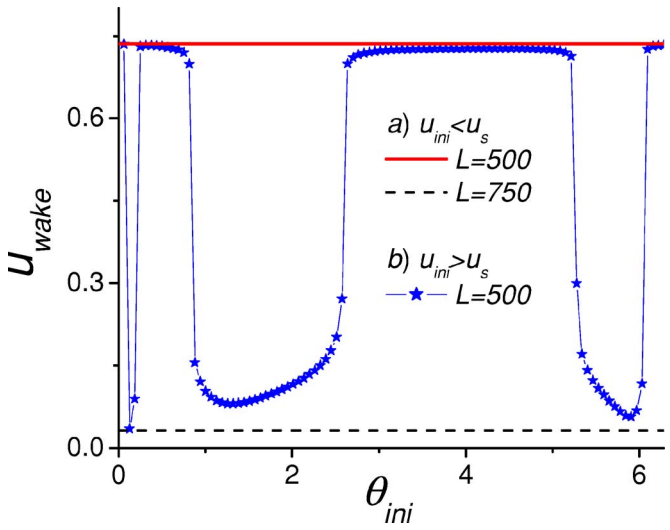

FIG. 9. (Color online) The wake amplitude u_{wake} vs initial phase θ_{ini} for different initial amplitudes u_{ini}: (a) $u_{ini} < u_s$ and (b) $u_{ini} > u_s$.

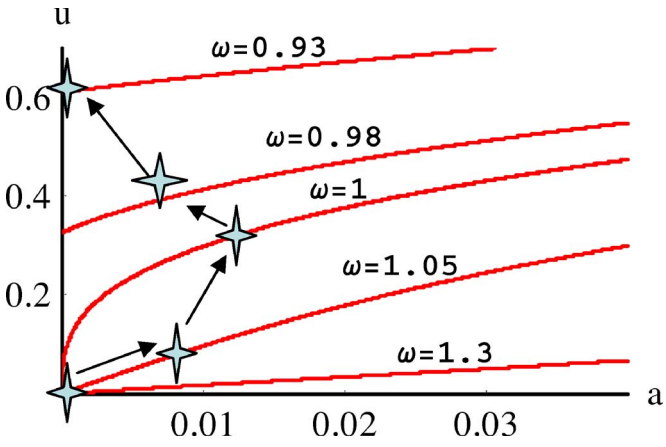

FIG. 10. (Color online) Red lines: the amplitude $u(\tau)$ of the upper elliptic point vs the driver amplitude a for different ω. Stars show the path of the upper elliptic point for varying detuning $b(\tau)$ and driver amplitude $a(\tau)$.

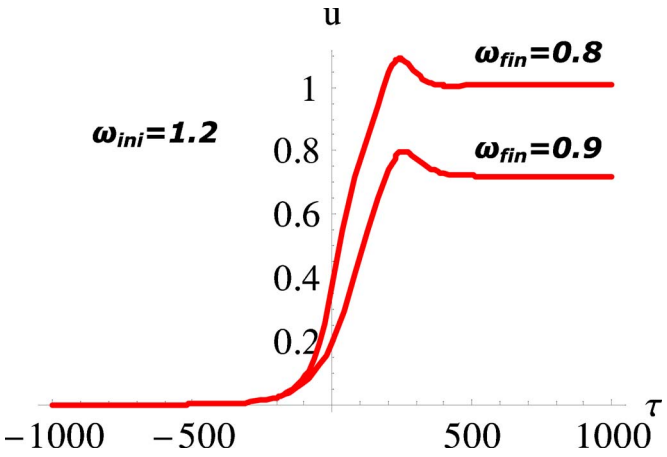

FIG. 11. (Color online) The oscillation amplitude vs normalized time for autoresonance. The driver pulse: $a(\tau)=a_m \exp(-\tau^2/\tau_L^2)$ with $a_m=0.012$ and $\tau_L=200$. The frequency chirp: linear from $\omega_{\rm ini}(-\tau_L)=1.2$ to $\omega_{\rm fin}(\tau_L)=0.8$ and 0.9.

tude $u_s \sim 1/\sqrt{2\tau_L}$, which corresponds to the initial adiabatic invariant $J_{\rm ini}$ of order of its "nonadiabatic" change during separatrix crossing.[17] It is seen from Figs. 8 and 9 that for the case $u_{\rm ini} < u_s$, the wake oscillation amplitude depends only on the driver pulse length τ_L and does not depend on the initial phase $\theta_{\rm ini}$ at all. Also, it is seen that the wake amplitude remains approximately the same for distinctly large regions of the driver pulse lengths and these regions are larger for the peak driver amplitude a_m close to the critical driver amplitude $a_{\rm cr}$ [the "flat-top" regions length is related to the periods given by Eq. (5), which tend to infinity close to the separatrix]. These remarkable properties of the wake allow one to easily control the bistable wake outcomes only by varying the driver (laser) pulse length. On the contrary, for $u_{\rm ini} > u_s$, the bistable outcomes start to depend on the initial phase, leading in turn to a highly unregular dependence of the wake amplitude on the driver pulse length. In this case, for random initial phases, the probabilities of each of the two bistable wake outcomes can be calculated by the method of Refs. 15, 17, and 19.

IV. AUTORESONANCE

Although the autoresonant mechanism of excitation of a large wake by varying the detuning (decreasing the driver frequency ω from or above the exact resonance frequency $\omega=1$) does not rely on the existence of the "sister" trajectories, it also can be explained in terms of the phase portraits of Hamiltonian (1). For the slow varying detuning $\omega(\tau)$ and driver amplitude $a(\tau)$ (the driver has the shape of the long adiabatic pulse), the autoresonance manifests itself in the phase locking of the initial oscillation with vanishing amplitude (quiescent plasma) to the upper elliptic point (UEP) of the Hamiltonian and subsequent adiabatic dragging of the phase-locked trajectory by the UEP. Indeed, for $b \le 0$ and vanishing driver amplitude a, the upper elliptic point has a vanishing amplitude (see Fig. 5), but with slow varying detuning (decreasing ω) and rising driver amplitude the UEP moves upwards in the phase space gradually acquiring a finite amplitude (see Figs. 4 and 10). The larger detuning is below the exact resonance (the smaller ω), the larger is the wake amplitude, as is shown in Fig. 11. Also, as is seen from Fig. 10, for large detuning below the resonance, the upper elliptic point has large amplitude even for the vanishing driver pulse amplitude (as is also seen from Fig. 1 for the elliptic point at $\theta=3\pi/2$). Actually, the wake amplitude for the autoresonance excitation from the quiescent initial state only depends on the final value of the "chirped" driver frequency $\omega_{\rm fin}$, and is given by $u_{\rm wake}=4\sqrt{(1-\omega_{\rm fin})/3}$. Also, the autoresonant wake amplitude is not sensitive to the driver and "chirp" shape, as long as the conditions of adiabaticity are met ($a/T_{\rm osc} \gg da/d\tau$ and $\omega/T_{\rm osc} \gg d\omega/d\tau$). Note that, although the adiabaticity conditions are inevitably broken for vanishing driver amplitudes [for $b>1$ and small driver amplitudes, the period of the phase-locked oscillations around UEP is $\sim 1/\sqrt{a}$)], this adiabaticity violation does not lead to noticeable changes of the oscillation amplitude, because in this case the driver is essentially turned off and cannot influence the oscillation energy and amplitude.

V. BISTABILITY WITH CHIRP

The autoresonant excitation of the large wake oscillation in the form described above (phase locking to the upper elliptic point) essentially relies on the "chirp" of the driver frequency downwards *from above*, $\omega_{\rm ini} > 1$, the linear resonance $\omega=1$. It turns out that the last condition can be relaxed and the large wake oscillation can be excited by bistability with chirp (or the "relaxed" autoresonance), even for the "chirp" starting *from below*, $\omega_{\rm ini} < 1$, the linear resonance, as is shown in Fig. 12. The mechanism of the bistability with chirp combines the main features of the bistability ("jumping" from the region of the lower elliptic point to the upper one and backwards with increasing and decreasing driver amplitude) and autoresonance ("dragging" of the trajectory encircling the upper elliptic point upwards in the phase plane with decreasing of the driver frequency). Indeed, for the bistability with chirp, initially, when $a \simeq 0$ and $\omega_{\rm ini} < 1$, the lower elliptic point (LEP) has vanishing amplitude, which results in phase-locking of the initial oscillation trajectory to

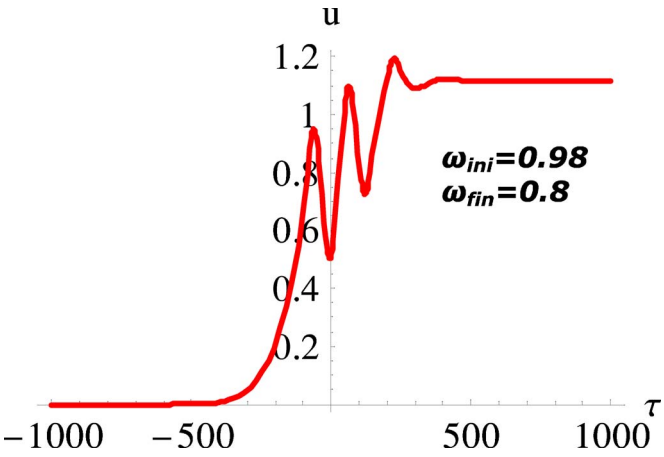

FIG. 12. (Color online) The oscillation amplitude vs normalized time for bistability with chirp. The driver pulse: $a(\tau)=a_m \exp(-\tau^2/\tau_L^2)$ with $a_m=0.012$ and $\tau_L=200$. The frequency chirp: linear from $\omega_{\text{ini}}(-\tau_L)=0.98$ to $\omega_{\text{fin}}(\tau_L)=0.8$.

it. Further on, as the driver amplitude increases and the driver frequency decreases, the LEP drags adiabatically the trajectory with itself upwards in the phase plane until a reaches the critical value a_{crit}. At this moment, the trajectory crosses the separatrix and starts to oscillate around the UEP. Further on, with still decreasing ω, the UEP moves upwards in the phase plane, adiabatically dragging the trajectory that oscillates around it without exact phase locking (the trajectory librates around UEP). When decreasing driver amplitude reaches the critical value a_{crit} again, the trajectory crosses the upper or lower part of the separatrix (depending on the oscillation phase) and adiabatically evolves to the wake value. Even if the trajectory crosses the lower part of the separatrix and moves into the region of the LEP, the wake oscillation still acquires the large amplitude as at this moment the driver frequency is essentially smaller than it was at the first separatrix crossing and tends to be even smaller for the subsequent times (see Fig. 12).

VI. CONCLUSION

In conclusion, a specific nonlinear resonant Hamiltonian with separatrix crossing, describing excitation of a nonlinear plasma wave in a plasma beat-wave accelerator, is analyzed. The Hamiltonian has a variable number of fixed points and can have the "sister" trajectories [multitrajectory solutions of $H(I,\theta)=h$], depending on the values of its parameters. The bistable evolution of the resulting dynamical system is analyzed and it is shown that in the adiabatic limit the Hamiltonian changes in the same way along the "sister" trajectories regardless of the multiple separatrix crossing. Also, it is shown that the bistable and autoresonant mechanisms of the excitation of a large wake amplitude are related to the properties of the resonant Hamiltonian and can be effectively used for generation of well-controllable wake oscillations.

[1] T. Tajima and J. M. Dawson, Phys. Rev. Lett. **43**, 267 (1979).
[2] M. N. Rosenbluth and C. S. Liu, Phys. Rev. Lett. **29**, 701 (1972).
[3] R. J. Noble, Phys. Rev. A **32**, 460 (1985).
[4] W. B. Mori, IEEE Trans. Plasma Sci. **PS-15**, 88 (1987).
[5] G. Shvets, Phys. Rev. Lett. **93**, 195004 (2004).
[6] W. M. Nevins, T. D. Ronglien, and B. I. Cohen, Phys. Rev. Lett. **59**, 60 (1987).
[7] I. A. Kotel'nikov and G. V. Stupakov, Phys. Fluids B **2**, 871 (1990).
[8] I. A. Kotel'nikov and G. V. Stupakov, J. Plasma Phys. **45**, 19 (1991).
[9] E. V. Suvorov and M. D. Tokman, Fiz. Plazmy **14**, 250 (1988).
[10] A. I. Neishtadt and A. V. Timofeev, Sov. Phys. JETP **66**, 973 (1987).
[11] S. Kalmykov, O. Polomarov, D. Korobkin, J. Otwinowski, J. Power, and G. Shvets, Philos. Trans. R. Soc. London, Ser. A **364**, 725 (2006).
[12] M. Deutsch, B. Meerson, and J. E. Golub, Phys. Fluids B **3**, 1773 (1991).
[13] R. R. Lindberg, A. E. Charman, J. S. Wurtele, and L. Friedland, Phys. Rev. Lett. **93**, 055001 (2004).
[14] L. D. Landau and E. M. Lifshitz, *Mechanics* (Pergamon, New York, 1976), p. 156.
[15] A. V. Timofeev, Sov. Phys. JETP **48**, 656 (1978).
[16] O. Polomarov and G. Shvets, Phys. Plasmas **13**, 054502 (2006).
[17] J. L. Tennyson, J. R. Cary, and E. F. Escande, Phys. Rev. Lett. **56**, 2117 (1986).
[18] I. S. Gradshteyn and I. M. Ryzhik, *Table of Integrals, Series, and Products* (Academic, New York, 1994), p. 290.
[19] J. R. Cary, D. F. Escande, and J. L. Tennyson, Phys. Rev. A **34**, 4256 (1986).